Radiology Case Reports 19 (2024) 4992–4999

Available online at www.sciencedirect.com

ScienceDirect

journal homepage: www.elsevier.com/locate/radcr

Case Report

Neuroimaging insights into poor prognosis paraneoplastic encephalomyelitis: A case report on a challenging diagnosis revealed by MR imaging in a patient with Hodgkin's lymphoma ☆

Abderrahmane Ibenyahia, MD[a,*], *Said Adnor, MD*[a], *Soufiane Bigi, MD*[a], *Imane Bazi, MD*[a], *Adel Elmekkaoui, MD*[b], *Benlenda Othmane, MD*[b], *Nassik Hicham, MD*[b], *Soukaina Wakrim, MD*[a]

[a] *Radiology Department, Faculty of Medicine and Pharmacy, University Hospital Center of Souss Massa, Ibn Zohr Agadir University, Agadir, Morocco*

[b] *Department of Anesthesia Reanimation, Faculty of Medicine and Pharmacy, University Hospital Center of Souss Massa, Ibn Zohr Agadir University, Agadir, Morocco*

ARTICLE INFO

Article history:
Received 8 July 2024
Revised 26 July 2024
Accepted 27 July 2024

Keywords:
Paraneoplastic Encephalomyelitis (PEM)
Hodgkin's lymphoma (HL)
Paraneoplastic neurological syndromes (PES)
Limbic Encephalitis (LE)
Rhombencephalitis
Magnetic resonance imaging

ABSTRACT

Paraneoplastic encephalomyelitis (PEM) is a rare complication associated with malignancies, often presenting before the cancer diagnosis. A 42-year-old male with a history of chronic smoking presented with acute urinary retention and neurological deficits, all evolving in a febrile context with general deterioration. Laboratory tests were conducted, followed by a cerebral MRI which revealed multiple T2 and FLAIR hyperintense lesions in the periventricular and periaqueductal regions, medial temporal lobes, and bilateral posteromedial thalamus. Enhanced CT scans of the chest and abdomen identified multiple cervical, axillary, and inguinal lymphadenopathies. Subsequently, an ultrasound-guided biopsy of a cervical node was performed. His condition deteriorated rapidly, requiring intubation and sedation. A subsequent MRI revealed worsening cerebral and spinal cord lesions with new contrast enhancement in the brainstem. The differential diagnosis included toxic/metabolic and paraneoplastic causes. Biopsy results confirmed Hodgkin's lymphoma, leading to a diagnosis of progressive paraneoplastic encephalomyelitis (PEM). Despite adequate treatment, the patient's condition worsened, leading to death from pneumonitis and metabolic complications. This case underscores the importance of considering PEM in patients with neurological deficits and malignancy, with MRI playing a crucial role in diagnosis. Early detection and treatment are essential to improving outcomes.

☆ Competing Interests: The authors declare no conflicts of interest regarding the publication of this article.

* Corresponding author.
E-mail address: abd.ibenyahia@gmail.com (A. Ibenyahia).

https://doi.org/10.1016/j.radcr.2024.07.159

Introduction

Paraneoplastic neurological syndromes (PNS) are rare but severe complications that occur in association with various malignancies, often presenting significant diagnostic challenges. Epidemiologically, PNS affects approximately around 1:300 patients with cancer [1], with Paraneoplastic encephalomyelitis (PEM) being one of the rarest manifestations. PEM is characterized by widespread neurological involvement and is frequently associated with small cell lung cancer, breast cancer, and Hodgkin's lymphoma. Diagnosing PEM is particularly challenging due to its nonspecific symptoms and the need for a multidisciplinary approach. Hodgkin's lymphoma, although primarily a lymphatic malignancy, can manifest in complex neurological syndromes, posing additional challenges for timely diagnosis and treatment [1].

This case highlights the importance of recognizing PEM in patients with neurological symptoms and a history of malignancy, emphasizing the critical role of MRI in diagnosis. Early detection and appropriate oncologic treatment are vital for improving patient outcomes.

Case presentation

A 42-year-old male with a history of chronic smoking (30 pack-years), cannabis use, and alcohol dependence, and reported consuming herbal products to aid in addiction cessation. The patient presented to the emergency department with a 3-day history of acute urinary retention, hematemesis, and progressive neurological deficits. On the third day, his symptoms notably worsened, especially the neurological manifestations. Neurological examination revealed marked paraparesis in the lower limbs, with muscle strength graded at 2/5, rendering the patient unable to stand or walk. Sensory examination was unremarkable, with normal proprioception, light touch, and vibration sense. Hyperreflexia was noted in the lower extremities with sustained clonus, while upper limb reflexes were normal. The patient also had hypertonic sphincters (urinary retention) and hyperalgesia. Examination of cranial nerves showed no abnormalities. All other neurological assessments, including upper limb motor function and coordination, were within normal limits. These symptoms all evolved in a febrile context leading to hospitalization. The patient's condition deteriorated rapidly, resulting in respiratory distress that required intubation and sedation.

Laboratory tests and radiologic imaging were conducted. A lumbar puncture showed clear cerebrospinal fluid with no albumin-cytological dissociation, glucose 0.49 g/L, proteins 0.20 g/L, chloride 121 mmol/L, 14 white blood cells (70% lymphocytic), and 14 red blood cells per mm^3. No pathogens were found on direct examination, and cultures were sterile after 48 hours. Blood tests revealed anemia (10.6 g/dL-8.2 g/dL), hyperleukocytosis (18,350 element/mcL), and platelet variation (from 98000 elements/mcL to 136000 elements/mcL). Hyponatremia correction over 8 days went from 117.5 mEq/L to 146 mEq/L, and fluctuating potassium levels (between 5.5 mEq/L and 4.6 mEq/L) were noted. Elevated liver enzymes (ASAT: 134 U/L, ALAT: 65.9 U/L) and C-reactive protein (between 128.8 mg/L and 131.2 mg/L) were observed, while renal function remained normal.

Initial cerebral MRI (Fig. 1) revealed multiple bilateral symmetrical lesions in the periventricular and periaqueductal regions, dorsomedial thalamus, medial temporal lobes, caudate, and brainstem. These lesions exhibited increased signal intensity on T2/FLAIR-weighted images and diffusion restriction with decreased ADC values. Medullary MRI (Fig. 2) showed diffuse T2 hyperintensities in the cervical, dorsal, and lumbar spinal cord. A subsequent cerebromedullary MRI performed a few days later demonstrated an aggravation of the previous lesions and the appearance of new lesions in the lenticular nuclei. There was a notable worsening of brainstem lesions with patchy contrast enhancement observed in the cerebral peduncles, superior cerebellar peduncles, superior colliculus, right side of the pons, and bilaterally in the medulla oblongata (Figs. 3 and 4). Additionally, there was more extensive bilateral symmetric FLAIR hyperintensity in the medial temporal lobes, periventricular white matter, and an extension of the spinal cord diffuse lesions seen in T2 and STIR sequences (Fig. 5). Enhanced CT scans revealed lymphadenopathy in the bilateral cervical and axillary regions and a left inguinal lymphadenopathy with marked infiltration in the para- and perirenal spaces bilaterally (Fig. 6).

These imaging findings are consistent with reported cases of PEM in the literature, which typically show symmetrical T2 hyperintensities and restricted diffusion. The involvement of multiple regions, such as the periventricular, periaqueductal, and medial temporal lobes, along with the brainstem and spinal cord, highlights the widespread nature of PEM. The patchy contrast enhancement observed in the follow-up MRI is also characteristic of the progressive nature of the disease. Enhanced CT scans revealing lymphadenopathy further support the diagnosis of an underlying malignancy, which is consistent with the literature describing similar imaging features in cases of PEM associated with Hodgkin's lymphoma.

Given the clinical, biological, and radiological presentation, we considered a toxic/metabolic origin due to the symmetric lesions and the patient's history, or a paraneoplastic encephalomyelitis given the presence of cervical, axillary, and inguinal lymphadenopathies. An ultrasound-guided biopsy performed on a cervical lymph node revealed dense and diffuse lymphoid infiltrates with eosinophilic necrosis. Immunohistochemical staining was positive for CD20 on reactive B lymphocytes, CD5 and CD3 on numerous reactive T lymphocytes, and CD30, CD15, Ki67, and PAX5 on large tumor cells, confirming a diagnosis of mixed cellularity classical Hodgkin's lymphoma (Fig. 7).

Following the pathological results, we diagnosed secondary paraneoplastic encephalomyelitis due to Hodgkin's lymphoma. Despite adequate treatment, including empiric intravenous antibiotics for pneumonitis and treatment for metabolic disorders, the patient's condition continued to worsen, leading to severe metabolic disorders and pneumonitis, resulting in a poor prognosis.

Following hospitalization and treatment, including antibiotics and management of metabolic disorders, the patient's condition continued to deteriorate. The initial presentation of urinary retention, hematemesis, and progressive neurological

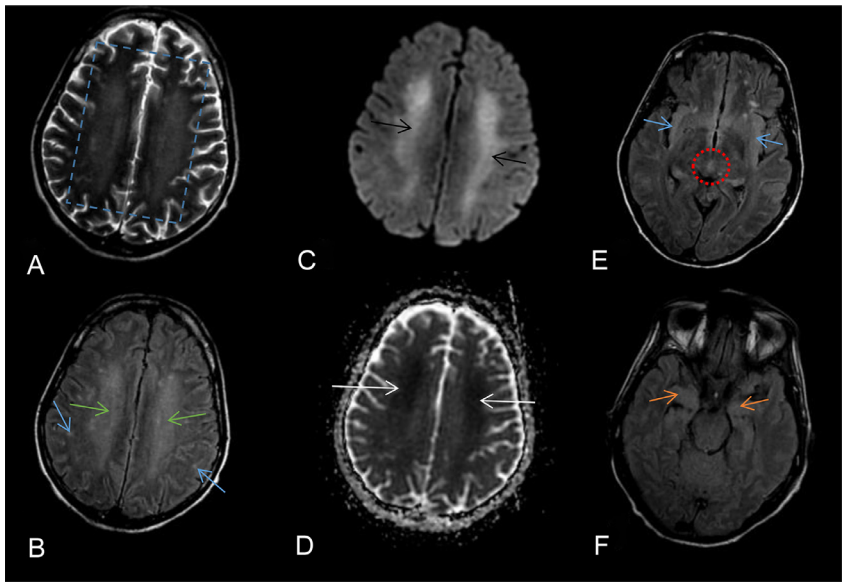

Fig. 1 – Initial MRI images axial different sequences showing. (A) Axial T2 weighted image showing increased signal in the periventricular and semi oval center bilaterally and symmetrically (blue dashed borders). (B) Axial FLAIR sequence showing increased signal in the periventricular and semi oval center bilaterally and symmetrically (green arrows) with some nodular and indeterminate hyperintensities (blue arrows). (C) Diffusion weighted imaging (DWI) showing restriction in the semi oval center bilaterally and symmetrically (black arrows). (D) decreased ADC values in the semi oval center diffusion restricted lesions bilaterally and symmetrically (white arrows). (E) axial FLAIR sequence showing hyperintensity bilateral and symmetrical in the insular (blue arrows) and peri aqueductal (red dashed circle). (F) axial FLAIR sequence showing symmetrical bilateral in medial temporal lobes and brainstem involvement (orange arrows).

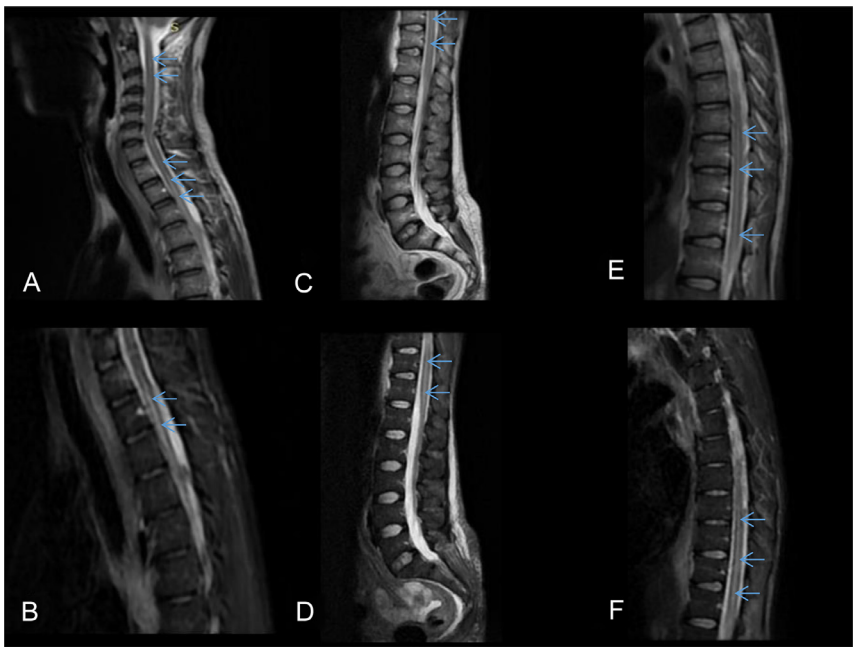

Fig. 2 – Initial medullar MRI sagittal T2 and STIR weighted images. (A) Sagittal T2 weighted image showing diffuse increased signal in the cervical and dorsal spinal cord (blue arrows). (B) Sagittal T2 STIR sequence image showing linear and diffuse increased signal in the dorsal spinal cord (blue arrows). (C) Sagittal T2 weighted image showing diffuse increased signal in the dorsolumbar spinal cord (blue arrows). (D) Sagittal T2 STIR sequence showing diffuse increased signal in the dorsolumbar spinal cord (blue arrows). (E) Sagittal T2 weighted image showing diffuse increased signal in the dorsal spinal cord (blue arrows). (F) Sagittal T2 STIR sequence showing diffuse increased signal in the dorsal spinal cord (blue arrows).

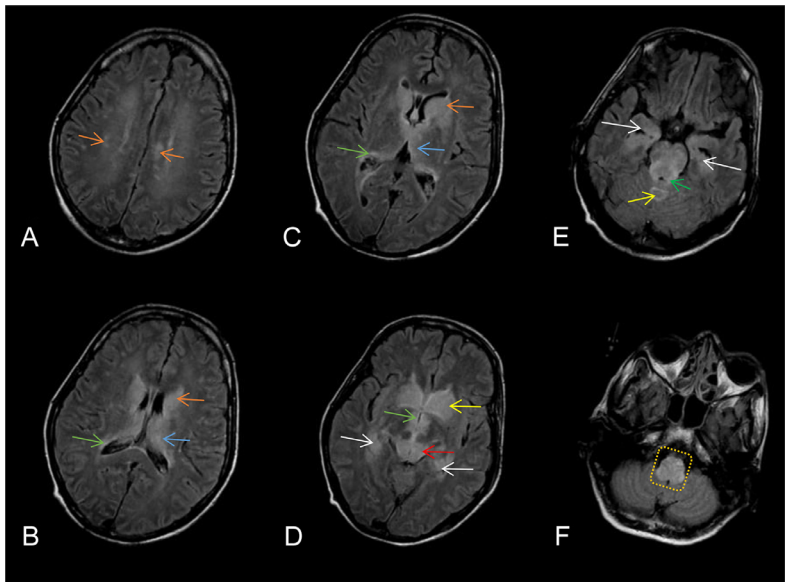

Fig. 3 – Follow up cerebral MRI FLAIR sequence images showing increased signal lesions. (A) Worsened periventricular nodular hyperintensities becoming confluent (orange arrows). (B) Aggravation of the periventricular (green arrow), postero medial thalamus (blue arrow) and caudate lesions (orange arrow) bilaterally and symmetrically. (C) Aggravation of the periventricular (green arrow), postero medial thalamus (blue arrow) and caudate lesions (orange arrow) bilaterally and symmetrically. (D) Lenticular (yellow arrow), periventricular (green arrow), posteromedial temporal lobes (white arrows) and cerebral peduncles (red arrow) lesions bilaterally and symmetrically. (E) Medial temporal lobes (white arrows), cerebellar superior peduncles (yellow arrow) and colliculus (green arrow) bilaterally and symmetrically. (F) Aggravation of the medulla oblongata lesion (orange dashed borders).

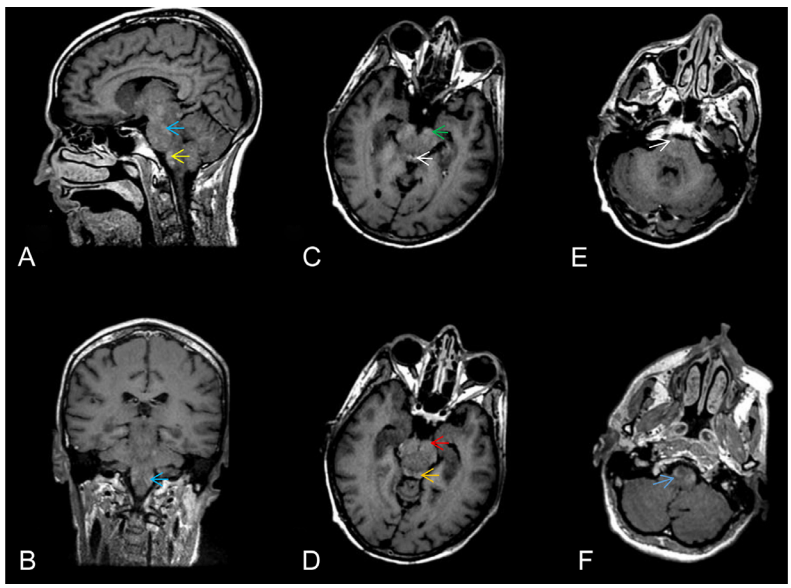

Fig. 4 – (A) Sagittal enhanced T1 spine echo sequence image showing the patchy contrast enhancement in the bulbar (yellow arrow) and pontine (blue arrow) regions. (B) Coronal enhanced T1 spine echo sequence image showing the patchy contrast enhancement in the bulbar region (blue arrow). (C) Axial enhanced T1 spine echo sequence image showing punctiforme contrast enhancement in the periaqueductal white matter (white arrow) and the cerebral peduncles (green arrow) bilaterally and symmetrically. (D) Axial enhanced T1 spine echo sequence image showing punctiforme contrast enhancement in the inferior colliculus (orange arrow) and the peduncles (red arrow) bilaterally and symmetrically. (E) Axial enhanced T1 spine echo sequence image showing a punctiforme contrast enhancement in the left side of the pons (white arrow). (F) Axial enhanced T1 spine echo sequence image showing punctiforme contrast enhancement in the medulla oblongata (tubercul cuneiforme) (blue arrow) bilaterally and symmetrically.

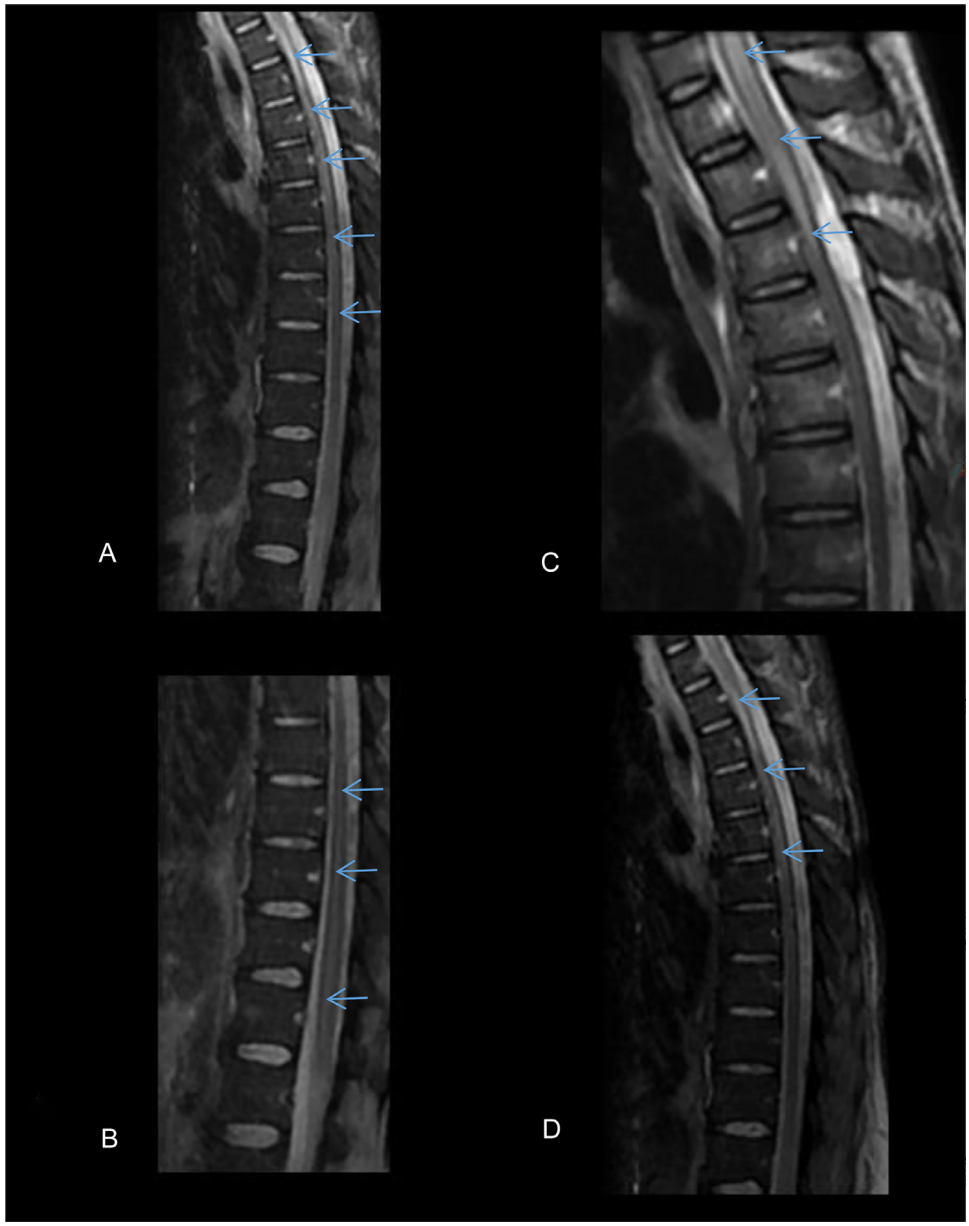

Fig. 5 – Medullar MRI follow up STIR T2 and T2 weighed images in sagittal plans. (A) Sagittal T2 STIR sequence image showing diffuse increased signal in dorsal spinal cord (blue arrows). (B) Sagittal T2 STIR sequence image showing linear and diffuse increased signal in the dorsolumbar spinal cord (blue arrows)
(C) Sagittal T2 weighted image showing the aggravation of the diffuse increased signal in the upper dorsal spinal cord (blue arrows). (D) Sagittal T2 STIR sequence showing the aggravation of the diffuse increased signal in the spinal cord (blue arrows).

deficits worsened, leading to respiratory distress. Ultimately, the patient succumbed to complications from infection and metabolic imbalances.

Discussion

Paraneoplastic encephalomyelitis (PEM) is a rare but critical condition associated with malignancies, including Hodgkin's lymphoma [1]. Paraneoplastic neurological syndromes (PNS) result from an autoimmune response triggered by an underlying malignancy, leading to neuronal dysfunction and inflammation. According to Graus et al. [2], diagnostic criteria for PNS include the presence of a neurological syndrome of unclear etiology, detection of well-characterized onconeural antibodies, and the presence of cancer. The application of these criteria can lead to early identification and treatment of the underlying tumor, which is crucial for managing PNS. MRI is the key examination that aids in diagnosing PNS and considering this diagnosis due to its ability to reveal characteristic imaging findings that are critical for accu-

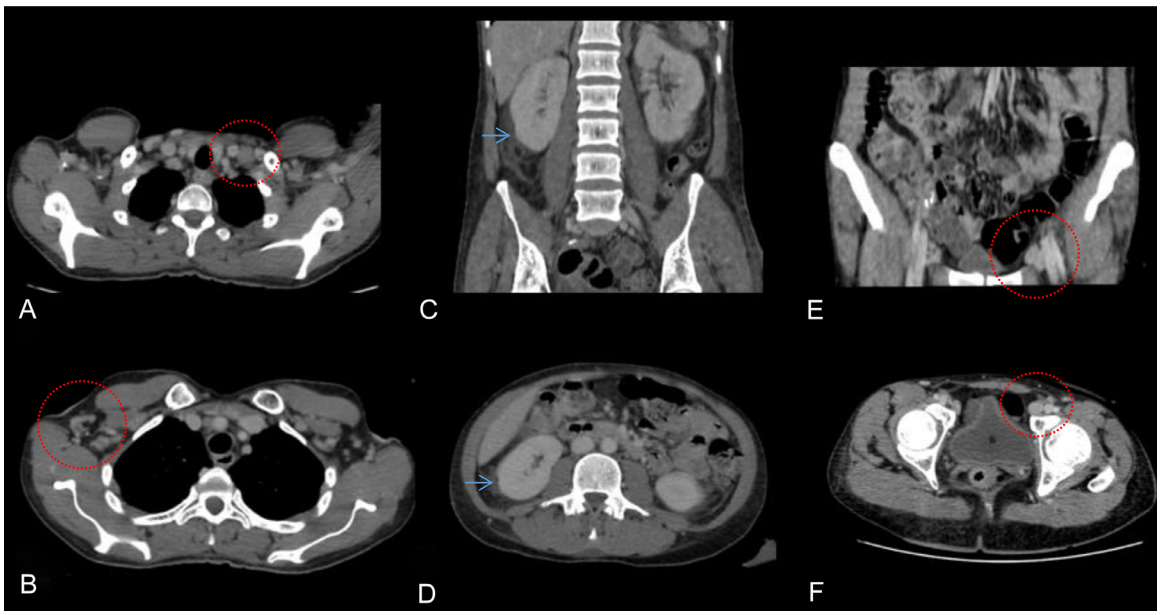

Fig. 6 – Enhanced CT reveals. (A) Axial plane showing lymphadenopathy left lower cervical of the medial supracalivcular level (IVb) (dotted red circle). (B) Axial plane showing lymphadenopathy right axillar region (dotted red circle). (C) Coronal plan showing the peri renal infiltration (blue arrow). (D) Axial plan showing the peri renal infiltration (blue arrow). (E) Coronal plan showing the left inguinal lymphadenopathy (dotted red circle). (F) Axial plan showing the left inguinal lymphadenopathy (dotted red circle).

IMMUNOHISTOCHIMIE

-Anticorps anti- CD20 (Clone L26, Bio SB):
Positif sur les lymphocytes B réactionnels.

-Anticorps anti- CD5 (Clone RBT-CD5, Bio SB):
Positif sur les nombreux lymphocytes T réactionnels.

-Anticorps anti- CD30 (clone Ber-H2, Bio SB):
Positif sur les cellules tumorales de grande taille.

-Anticorps anti-Ki67 (Clone SP6, Thermoscientific):
Positif sur les cellules tumorales de grande taille.

-Anticorps anti- Pan-cytokératine (Clone AE1/AE3, Bio SB):
Négatif.

-Anticorps anti-CD3 (Clone RBT-CD3e, Bio SB):
Positif sur les nombreux lymphocytes T.

-Anticorps anti- CD15 (Clone MMA, Bio SB):
Positivité des cellules tumorales de grande taille.

-Anticorps anti-PAX 5 (Clone RBT-PAX5, Bio SB):
Positivité des cellules tumorales de grande taille.

-Anticorps anti- ALK 1 (Clone RBT, ALK-1, Bio SB):
Négatif.

-Anticorps anti- Granzyme B (Clone Polyclonal, Bio SB):
Négatif.

CONCLUSION :
-Aspect immunohistochimique d'un lymphome de Hodgkin classique à cellularité mixte.

Fig. 7 – Immunohistochemistry staining results.

rate identification and differentiation from other pathologies. PNS can manifest as various syndromes, including limbic encephalitis, brain stem encephalitis (rhombencephalitis), and myelitis.

Limbic encephalitis involves inflammatory changes in the limbic system, including the hippocampus, amygdala, hypothalamus, and cingulate cortex. Symptoms include mood and behavioral changes, cognitive dysfunction, memory loss, and seizures [3]. Imaging typically shows T2 hyperintensity and swelling of the mesial temporal lobes [4]. Differential diagnosis includes herpes simplex viral encephalitis, status epilepticus, neurosyphilis, and glioma [5].

Brain stem encephalitis predominantly affects the brain stem but can also involve the cerebellar peduncles and hemispheres. Clinical presentation may include ataxia, dysarthria, and ophthalmoplegia. Imaging findings vary with disease progression, initially showing T2 hyperintensity and/or enhancement of the affected areas, which can later lead to atrophy [6].

Paraneoplastic myelitis is characterized by inflammation of the spinal cord, presenting with symptoms such as weakness, numbness, and bowel or bladder dysfunction [4]. Imaging reveals longitudinally extensive T2 hyperintensity and enhancement, often affecting the lateral columns [7].

In our case, the combination of clinical presentation, biological markers, and radiological findings strongly suggested a diagnosis of PEM, particularly reinforced by the biopsy results and subsequent MRI findings. Regular MRI follow-up is crucial to prevent diagnostic errors and ensure accurate monitoring of the disease progression [8]. The imaging characteristics of limbic encephalitis, rhombencephalitis, and myelitis in our case were distinct and consistent with those described in medical literature. Immunohistochemical staining confirmed a diagnosis of classical Hodgkin's lymphoma. These findings led to a diagnosis of progressive paraneoplastic encephalomyelitis.

Paraneoplastic encephalomyelitis (PEM) treatment focuses on managing the underlying malignancy and using immunotherapy like corticosteroids, IVIG, and plasmapheresis. Early intervention is crucial for better outcomes [9]. Combining cancer treatment with immunotherapy improves neurological outcomes and survival [6]. Despite treatment, our patient's condition worsened, highlighting the aggressive nature of PEM and the need for timely intervention.

Prognosis for patients with PEM depends on several factors, including the timeliness of diagnosis, the effectiveness of treatment, and the extent of neurological involvement. Early diagnosis and prompt treatment of the underlying malignancy can significantly improve patient outcomes. However, delayed diagnosis and treatment are associated with poor prognosis, as seen in our case where the patient's condition deteriorated rapidly, leading to severe metabolic disorders and pneumonitis.

This case underscores the importance of MRI in diagnosing PEM and differentiating it from other conditions. Radiologists must recognize the characteristic imaging features of PEM and consider it in the differential diagnosis for patients with neurological symptoms and a history of malignancy. Rapid biopsy and immunohistochemical analysis are essential for confirming the diagnosis and guiding treatment [10]. Despite adequate treatment, the patient's condition deteriorated, leading to a fatal outcome from pneumonitis and metabolic complications.

Conclusion

Paraneoplastic encephalomyelitis is a rare but severe condition associated with Hodgkin's lymphoma, where MRI plays a crucial role in diagnosis. Early consideration of PEM in differential diagnosis, rapid biopsy, and confirmation of the malignancy allows for timely treatment, significantly improving outcomes. This case underscores the need for a high index of suspicion and proactive management in patients with neurological symptoms and a history of malignancy. Clinical recommendations include considering PEM in differential diagnosis, using MRI to identify characteristic findings, performing regular MRI follow-ups, conducting rapid biopsies and immunohistochemical analyses, and initiating immunosuppressive therapy promptly. This highlights the importance of a multidisciplinary approach involving radiologists, neurologists, and oncologists for comprehensive care.

Patient consent

Written informed consent was obtained from the patient's family for the writing and publication of this article and accompanying images.

REFERENCES

[1] Briani C, Vitaliani R, Grisold W, Honnorat J, Graus F, Antoine JC, et al. PNS Euronetwork. Spectrum of paraneoplastic disease associated with lymphoma. Neurology 2011;76(8):705–10.
[2] Graus F, Delattre JY, Antoine JC, Dalmau J, Giometto B, Grisold W, et al. Recommended diagnostic criteria for paraneoplastic neurological syndromes. J Neurol Neurosurg Psychiatry 2004;75(8):1135–40.
[3] Kelley BP, Patel SC, Marin HL, Corrigan JJ, Mitsias PD, Griffith B. Autoimmune encephalitis: Pathophysiology and imaging review of an overlooked diagnosis. AJNR Am J Neuroradiol 2017;38:1070–8.
[4] Guerin J, Watson RE, Carr CM, Liebo GB, Kotsenas AL. Autoimmune epilepsy: Findings on MRI and FDG-PET. Br J Radiology 2019;92:20170869.
[5] da Rocha AJ, Nunes RH, Maia AC, do Amaral LL. Recognizing autoimmunemediated encephalitis in the differential diagnosis of limbic disorders. AJNR Am J Neuroradiol 2015;36:2196–205.
[6] Madhavan AA, Carr CM, Morris PP, Flanagan EP, Kotsenas AL, Hunt CH, et al. Imaging review of paraneoplastic neurologic syndromes. AJNR Am J Neuroradiol 2020;41:2176–87. doi:10.3174/ajnr.A6815 2176.
[7] Keegan BM, Flanagan EP. In reply—Sensitivity of [18F]-fluorodeoxyglucose-positron emission tomography in patients with active myelopathy. Mayo Clin Proc 2014; 89:859.

[8] Rutherford GC, Dineen RA, O'Connor A. Imaging in the investigation of paraneoplastic syndromes. Clin Radiol 2007;62(11):1021–35.
[9] Josep O, Dalmau MD, Jerome B, Posner MD. Paraneoplastic syndromes neurological review. Arch Neurol 1999;56:405–8.
[10] Badawy M, Revzin MV, Consul N, Soliman M, Ganeshan DM, Heymann JC, et al. Paraneoplastic syndromes from head to toe: Pathophysiology, imaging features, and workup. Radiographics 2023;43(3):e220085. doi:10.1148/rg.220085.